Available online at www.sciencedirect.com
SCIENCE DIRECT®
Polymer 44 (2003) 3545–3551
polymer
www.elsevier.com/locate/polymer

Parallel processes in the recovery of biaxially oriented amorphous polymer films

C.C. Chau[a,*], J.C.M. Li[b]

[a]*The Dow Chemical Company, Midland, MI, USA*
[b]*University of Rochester, Rochester, NY, USA*

Received 28 October 2002; received in revised form 2 February 2003; accepted 5 February 2003

Abstract

The dimensional recovery of biaxially oriented styrene–acrylonitrile (SAN) copolymer films appears to consist of two second-order kinetic processes taking place in parallel. The earlier stage of recovery is dominated by a second-order process with a higher rate constant and a lower activation energy. The later stage process has a lower rate constant but with a higher activation energy. In the earlier stage, the recovery of length (machine direction) and width (transverse direction) appears to take place in parallel so that the rate constant of area recovery can be approximated as the sum of those of the length and width recoveries. In the later stage, the recovery of length and width appears to take place consecutively so that the rate constant of area recovery is the harmonic mean of those of the length and width recoveries. These findings suggest two types of conformational motion incurred simultaneously during annealing: one involves large scale chain motions that take place at the earlier stage and the other involves small scale chain motions that take place at the later stage. The large scale chain motions which govern the length and width recovery appear to occur independently, but the small scale motions appear to take place consecutively.

Keywords: Polystyrene; Recovery; Kinetics

1. Introduction

Biaxial orientation is known to significantly affect the physical properties of a polymer. The tensile strength and modulus of the oriented films show dramatic increases over the non-oriented materials [1,2]. For oriented styrene–acrylonitrile copolymer films, both the machine direction (MD) and transverse direction (TD) show strong ductility and hardening behavior upon tensile deformation. Shear banding, rather than crazing, prevails in the tensile yielding process [3]. These observations indicate that biaxial deformation greatly changes the state of an amorphous polymer.

A biaxially oriented film can change its linear dimensions upon annealing above the glass transition temperature of the polymer. Previous studies have shown that the linear dimensions can recover to a non-oriented state after sufficient annealing [4]. It has also been shown that the kinetics of recovery followed second order for the later part of the recovery process, suggesting the possibility of defect annihilation during annealing [5].

In this study, both the earlier and later stages of the recovery were analyzed by considering simultaneous large scale and small scale chain motions. The recovery data were examined and analyzed in the light of two second-order kinetic processes. An analysis of the data for the two biaxial directions and the area defined by the two directions provided detailed understanding of the two processes governing the length and width recoveries.

2. Experimental

2.1. Materials and sample preparation

The styrene–acrylonitrile random copolymer used in this study was produced by The Dow Chemical Company. It contained 70% styrene and 30% acrylonitrile with a glass transition temperature (T_g) of 102 °C and a weight average molecular weight of 185,000. Biaxially oriented films about

* Corresponding author.

0032-3861/03/$ - see front matter © 2003 Elsevier Science Ltd. All rights reserved.
doi:10.1016/S0032-3861(03)00162-9

28 μm thick were made through a controlled orientation process. Materials in pellet form were extruded in a Killion extruder and subsequently blown in a blown film bubble process. The degree of orientation along the MD was higher than that of the TD. The optically clear films were air-cooled and packed in rolls of 28 cm wide with the length direction being the MD. Specimens, 80 mm × 80 mm, were razor-cut from the roll with the edges parallel to the MD and TD.

2.2. Annealing and dimensional measurements

Specimens were laid flat on 'Kim-Wipe' papers put on a glass plate preheated in a Fisher Isotemp forced air oven at a chosen setting before the experiments. The oven was modified with a model 2002 process controller from LFE Corporation for precise temperature control and resolution (0.1 °C). Specimens were annealed at a temperature higher than T_g for a chosen time period, removed from the oven for dimensional measurements, and returned to the oven for another period of annealing. The initial length (MD) and width (TD) of the films were measured by a conventional flexible ruler along each of the four sides. The thickness of the film was monitored by using a Brown and Sharp micrometer capable of resolving 0.1 mil (2.54 μm). After the first annealing time period, the length and width of the films were also measured by using the micrometer. An average of five measurements was taken for each recording on the same side of the sample.

3. Results and discussion

3.1. Recovery kinetics

Second-order kinetic processes were proposed in the recovery of shear bands, the volumetric recovery of polystyrene [6] and the recovery of deformed polymers [7]. In the previous study [4], the recovery of biaxially oriented SAN films was also found to follow second order for the later stage of the process. For most of these previous studies, the initial part of the recovery was not found to fit by a single second-order process that was used for fitting the later stage of recovery.

In this study, two processes are proposed in the deformation and recovery of an amorphous polymer. One is related to the large scale chain motion such as sliding between main chains. The other is related to a small scale chain motion such as rotation or bending of a side group [5]. When a polymer is deformed, both processes could take place simultaneously. Energies can then be stored with the introduction of twists and bends in the molecules. These twists and bends could carry opposite signs, such as groups with opposite twist directions [5], and distributed over the deformed region. A possible mechanism of recovery is to eliminate such twists and bends toward equilibrium corresponding to the undeformed state. The kinetics of the elimination of twists and bends that carry opposite signs should then be second order with the change in dimension proportional to the concentration of these twists and bends.

By assuming that the linear dimensional change is proportional to the concentration of the twists and bends, the recovery can be examined in terms of the dimensional variations. The second-order rate relationships for the two processes can be expressed as follows:

$$\frac{\mathrm{d}}{\mathrm{d}t}\left(\frac{x_1}{x_{1\mathrm{o}}}\right) = -k_1\left(\frac{x_1}{x_{1\mathrm{o}}}\right)^2 \tag{1}$$

$$\frac{\mathrm{d}}{\mathrm{d}t}\left(\frac{x_2}{x_{2\mathrm{o}}}\right) = -k_2\left(\frac{x_2}{x_{2\mathrm{o}}}\right)^2 \tag{2}$$

where x_1 and x_2 represent the part of linear dimensions for the two processes, respectively, k_1 and k_2 are rate constants for the two recovery processes. The total dimension, x, at any time t is:

$$x = x_1 + x_2 + x_\infty \tag{3}$$

and at $t = 0$

$$x_\mathrm{o} = x_{1\mathrm{o}} + x_{2\mathrm{o}} + x_\infty \tag{4}$$

where x_∞ represents the final dimension which is not recoverable, x_o represents the initial dimension which includes the initial dimensions of the two processes, $x_{1\mathrm{o}}$ and $x_{2\mathrm{o}}$ at $t = 0$.

3.2. Kinetics of length, width and area recovery

Fig. 1(a) and (b) shows the recovery of length (MD) and width (TD) of SAN film samples annealed at temperatures ranging from 106 to 118 °C, respectively (data from Ref. [4]). The length decreased rapidly at the earlier stage of annealing and leveled off at long annealing times. The rate of decrease appears to be changing rapidly with temperature. These recovery data were analyzed by using the proposed dual second-order kinetic processes as shown in Eqs. (1)–(3).

The second-order rate relationships as shown in Eqs. (1) and (2) yielded the following results:

$$\frac{x_{1\mathrm{o}}}{x_1} = 1 + k_1 t \tag{5}$$

$$\frac{x_{2\mathrm{o}}}{x_2} = 1 + k_2 t \tag{6}$$

where x_1 and x_2 represent the linear dimensions along the length (L) or the width (W) of the film, respectively; x_1 and x_2 are represented by L_1 and L_2 for length recovery, or W_1 and W_2 for width recovery in the following descriptions.

The fitting of the data with the dual second-order equations was performed in Microsoft Excel by using the Solver function. Four parameters, k_1, k_2, x_∞ and $x_{1\mathrm{o}}$ were resolved from Eqs. (3)–(6) with $x_{2\mathrm{o}}$ being a dependent parameter. The fitting was performed by minimizing the summation of the logarithmic differences between the

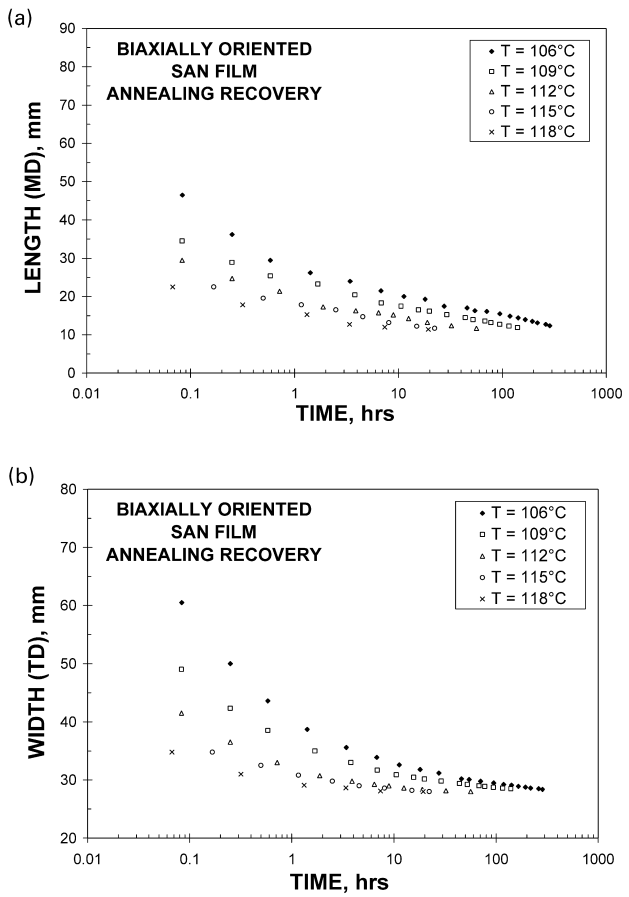

Fig. 1. (a) The variation of the length (MD) of SAN films with time upon annealing. (b) The variation of the width (TD) of SAN films with time upon annealing.

measured and the calculated dimensions for each measurement. Fig. 2 shows an example of the best fit for width recovery at 106 °C. The two second-order relationships used in this fit were

$$\frac{W_{1o}}{W_1} = 1 + k_{W1}t \tag{7}$$

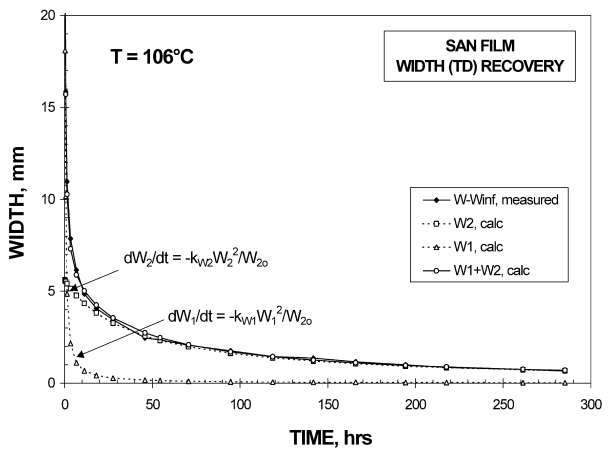

Fig. 2. An example of the fitting of the dual second-order kinetic model for the recovery of the width (TD) annealed at 106 °C.

and

$$\frac{W_{2o}}{W_2} = 1 + k_{W2}t \tag{8}$$

The two second-order plots gave a $W_1 + W_2$ summation plot which fits well with the measured data $W - W_\infty$, where W_∞ is also a fitting parameter.

Fig. 3(a) and (b) shows the second-order plots in which $1/L_1$ and $1/L_2$ was plotted against time for the five temperatures. L_1 and L_2 are the fitted linear dimensions for the two second-order kinetic processes along the length direction (MD). The recovery can be represented by these two processes occurred simultaneously upon annealing. As shown in these plots, the second-order kinetics was obeyed throughout the recovery. L_1 represents a faster process that yields a rate constant ranging from approximately 10–252 h^{-1}, and L_2, a slower process with a much smaller rate constant which is in the range of approximately 0.01–1 h^{-1}.

The recovery of width was also examined based on the dual second-order kinetics as proposed. Again, the recovery can be characterized by considering two simultaneous processes. The resolved two second-order plots are shown in Fig. 4(a) and (b). The fast process has a larger rate constant

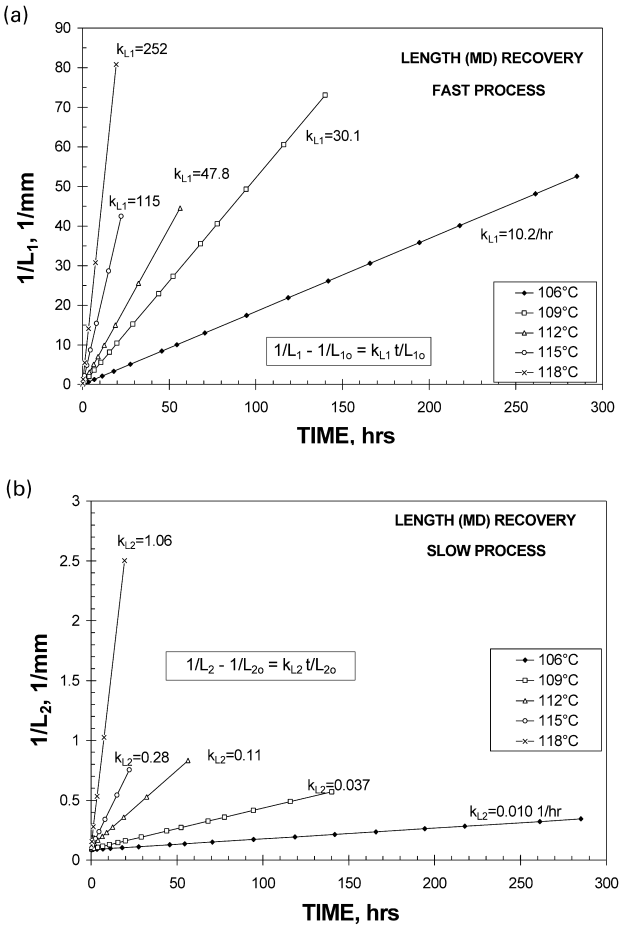

Fig. 3. (a) The resolved fast second-order kinetic process for the recovery of length (MD). (b) The resolved slow second-order kinetic process for the recovery of length (MD).

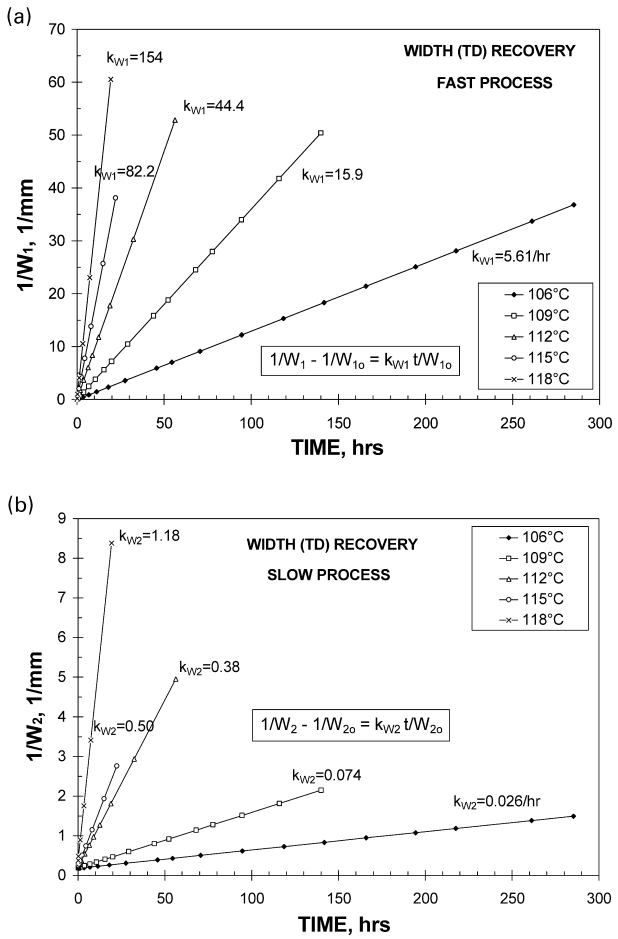

Fig. 4. (a) The resolved fast second-order kinetic process for the recovery of film width. (b) The resolved slow second-order kinetic process for the recovery of film width.

ranging from approximately 6–154 h^{-1}, and the slower process, 0.03–1.2 h^{-1}.

In this study, the recovery of film area as defined by the linear dimensions was also examined. The area data, obtained by length times width, is shown in Fig. 5 for samples annealed at temperatures ranging from 106 to 118 °C, respectively. By using the same fitting method, the

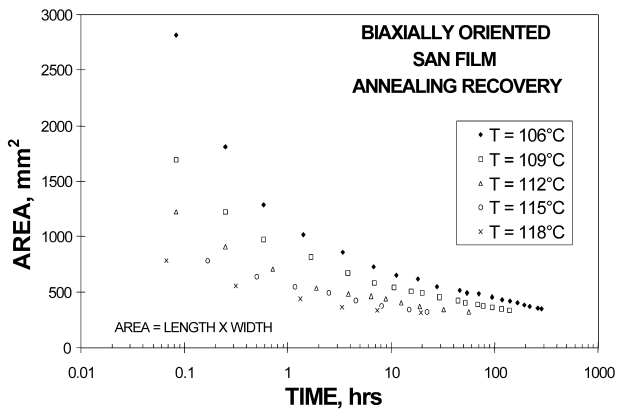

Fig. 5. The variation of film area (length × width) with time upon annealing.

area recovery data was also found to fit the dual second-order kinetics, one fast and one slow. Fig. 6(a) and (b) shows the second-order kinetics plots for the two processes. It is clear that second-order kinetics well represented the area recovery with the rate constant of the faster process ranging from approximately 15–422 h^{-1}, and that of the slower process, 0.02–1.2 h^{-1}.

The temperature dependence of the rate constants showed Arrhenius relationships as shown in Fig. 7(a) and (b) for the fast and slow processes, respectively. The activation energy for the fast process is approximately 331 ± 8 kJ/mol from the rate data of the length, width and area recovery. The fact that the three analyses revealed a narrow spread of the activation energy indicates that a single molecular process incurred in the recovery. The activation energy for the slow process as shown from the plot in Fig. 7(b) was approximately 440 ± 34 kJ/mol. This activation energy was smaller than that obtained previously from just the later stage analysis [4]. This is likely attributed to the fitting approximations used.

The fitted final unrecoverable dimensions, L_∞, W_∞ and A_∞ were obtained independently from individual fitting. Fig. 8 shows the data of $L_\infty \times W_\infty$ versus A_∞ for all the temperatures studied. It is found that the two

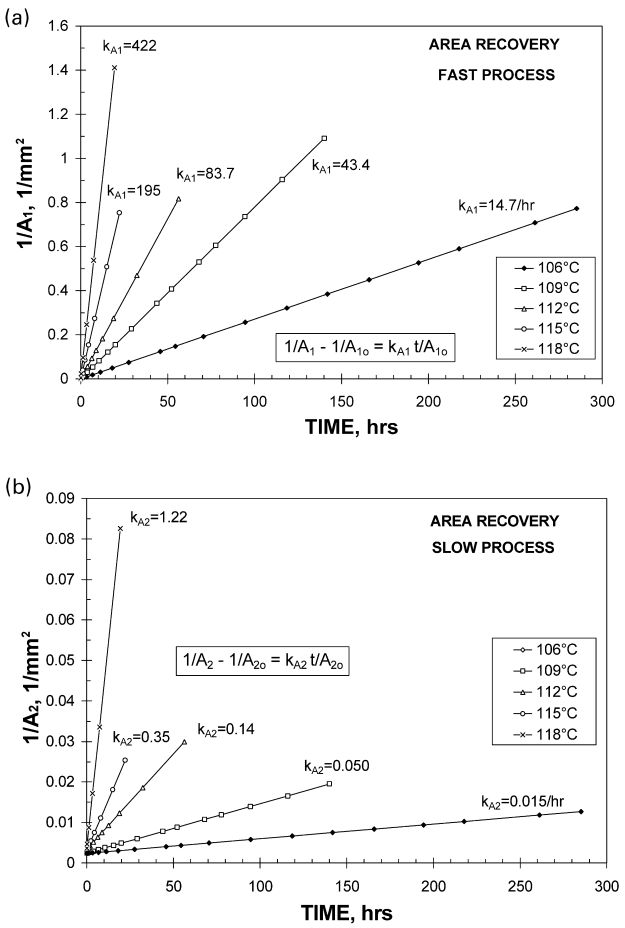

Fig. 6. (a) The resolved fast second-order kinetic process for area recovery. (b) The resolved slow second-order kinetic process for area recovery.

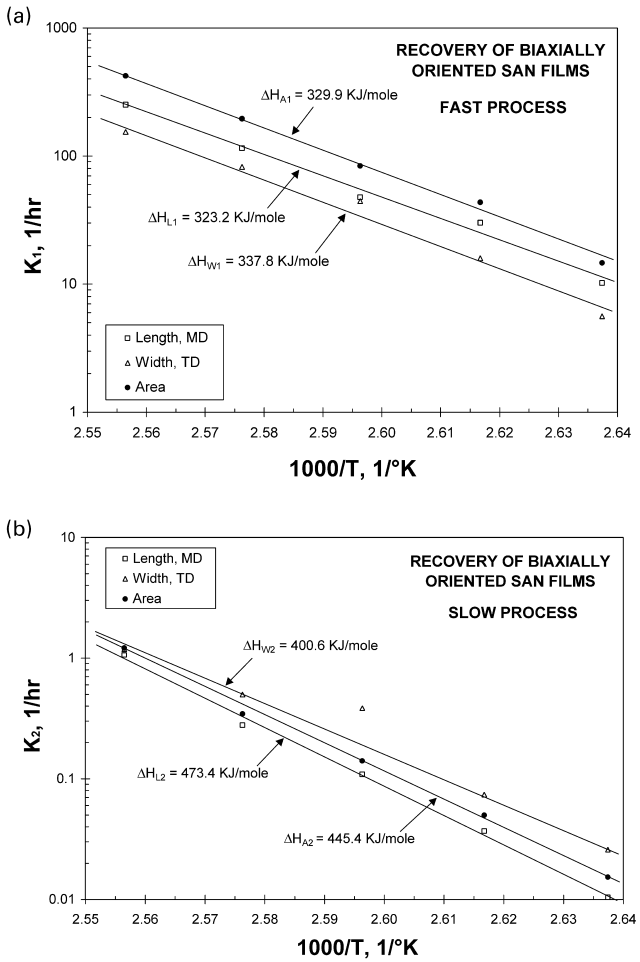

Fig. 7. (a) The Arrhenius relationship of the rate constant for the fast process. (b) The Arrhenius relationship of the rate constant for the slow process.

quantities were approximately equivalent. The difference was within 5% with most of the data within only 2%. The final dimensions represent the dimension that can only be achieved after infinite time of annealing. The equivalence of the $L_\infty \times W_\infty$ and A_∞ indicates the consistency of the fitting procedures.

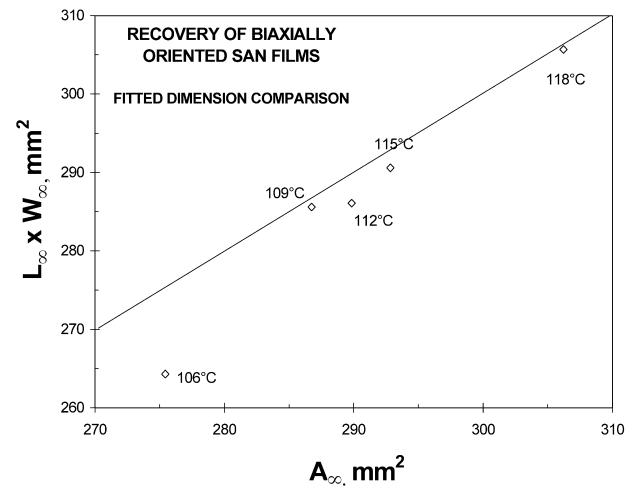

Fig. 8. Comparison for the fitted dimensions among length, width and area.

3.3. Parallel and consecutive processes in early and later stages of recovery

To understand their mutual interactions, the fitted dimensions and the rate relationships of recovery between length, width and area are further analyzed. The total initial film area A_o can be expressed by the following relationship:

$$A_o = A_{1o} + A_{2o} + A_\infty = L_o W_o$$

$$= (L_{1o} + L_{2o} + L_\infty)(W_{1o} + W_{2o} + W_\infty) \quad (9)$$

Here A_{1o} and A_{2o} represent the initial areas for the fast and slow processes, respectively. Since $A_\infty = L_\infty W_\infty$, A_{1o}, the area for the fast or the early stage process, can be expressed as:

$$A_{1o} = L_{1o} W_{1o} + W_{1o} L_o - L_{1o} W_{1o} \quad (10)$$

And the area for the slow or the later stage process, A_{2o}, can be expressed as:

$$A_{2o} = L_{2o} W_{2o} + L_{2o} W_\infty + W_{2o} L_\infty \quad (11)$$

The fitted dimensions of length, width and area for the two processes are summarized in Table 1. The two areas are also calculated by using Eqs. (10) and (11). Comparisons between the fitted and the calculated values are expressed as the percentages of the difference between the fitted and calculated areas divided by the fitted area values. It can be seen that a good agreement was obtained between the fitted and calculated area values with the differences mostly within 5%. This demonstrates that the proposed relationships among the dimensions appear to be valid.

During the recovery, the film area A is expressed as:

$$A = A_1 + A_2 + A_\infty = LW$$

$$= (L_1 + L_2 + L_\infty)(W_1 + W_2 + W_\infty) \quad (12)$$

In the beginning of recovery, L_1 and W_1 are the dominating quantities so that

$$A_1 \cong L_1 W_1 \quad (13)$$

Differentiating this equation with respect to time and note that in the very beginning $A_1 \cong A_{1o}$, $L_1 \cong L_{1o}$, and $W_1 \cong W_{1o}$. Hence to a first order approximation:

$$k_{A1} = k_{L1} + k_{W1} \quad (14)$$

The rate constant for the area recovery should be the summation of the rate constants for the length and the width recoveries. This shows that, in the early stage of recovery of area by two processes, one recovers the length and the other recovers the width. The faster one controls the rate of area recovery so that they take place in parallel.

For the later stage of recovery, $k_1 t$ is much larger than 1 in Eqs. (5) and (6) at long times and A_2 can be approximated

Table 1
A comparison between the fitted and calculated dimensions for length, width and area

T (°C)	L_{1o}	L_{2o}	W_{1o}	W_{2o}	A_{1o}	A_{2o}	A_{1o}, calc.	A_{2o}, calc.	A_{1o} % difference	A_{2o} % difference
106	55.30	11.56	43.49	5.61	5407	421.7	5166	438.8	4.46	4.07
109	57.61	10.87	44.29	5.29	5580	409.2	5404	415.9	3.15	1.64
112	60.43	8.58	47.34	4.57	5773	298.1	5717	325.4	0.97	9.16
115	60.14	9.53	47.99	4.37	5771	342.3	5764	350.1	0.13	2.29
118	60.42	8.60	49.29	2.86	5797	297.0	5798	295.5	0.01	0.53

from Eq. (11):

$$A_2 \cong W_2 L_\infty + L_2 W_\infty \tag{15}$$

Since

$$A_{2o} \cong L_{2o} W_{2o} \tag{16}$$

We have

$$\frac{1}{k_{A2}} = \frac{1}{k_{W2}}\left(\frac{L_\infty}{L_{2o}}\right) + \frac{1}{k_{L2}}\left(\frac{W_\infty}{W_{2o}}\right) \tag{17}$$

The rate constant for area recovery is the weighted harmonic mean of the rate constants for the recovery of the length and the width. This shows that in the later stage of recovery of area by two processes, one recovers the length and the other recovers the width. The slower one controls the rate. The recovery of length and width at the later stage is a consecutive process. They take place in steps alternating to each other.

The data for the early stage recovery is shown in Table 2 for a comparison between the three early stage rate constants, k_{A1}, k_{L1}, k_{W1}. The results show that the suggested relationship of Eq. (14) does seem to follow. The difference between k_{A1} and $k_{L1} + k_{W1}$ is mostly within 10% in the temperature range examined.

The analysis of the later stage data using the relationship of Eq. (17) is shown in Table 3 for the difference between $1/k_{A2}$ and $L_\infty/(k_{W2}L_{2o}) + W_\infty/(k_{L2}W_{2o})$. The agreement also seems satisfactory.

These observations and considerations indicate that the recovery of the biaxially oriented SAN films possesses two different mechanisms that operate independently throughout the annealing processes. The early stage process involves large scale chain motions and the later stage involves small scale chain motions. The two large scale motions corresponding to the length and width recovery in the early stage seem to operate in parallel. However, the two small scale motions corresponding to the length and width recovery in the later stage occur consecutively one after the other.

Table 2
Examination of the rate relationship among k_{L1}, k_{W1} and k_{A1} for the early stage recovery

T (°C)	k_{A1} (h^{-1})	k_{L1} (h^{-1})	k_{W1} (h^{-1})	$k_{L1} + k_{W1}$ (h^{-1})	% difference
106	14.65	10.19	5.611	15.80	7.9
109	43.44	30.06	15.93	45.99	5.9
112	83.68	47.78	44.40	92.18	10.2
115	195.4	114.8	82.16	197.0	0.81
118	422.1	251.9	153.9	405.8	3.9

4. Summary and conclusions

(1) The recovery of length, width and area of biaxially oriented films appeared to follow two second-order kinetic processes that take place in parallel during thermal annealing.
(2) The earlier stage recovery is dominated by a faster process with a higher rate constant (10–252 h^{-1}) and a lower activation energy (331 ± 8 kJ/mol). The later stage recovery is dominated by a slower process with a smaller rate constant (0.01–1 h^{-1}) and a higher activation energy of approximately 440 ± 34 kJ/mol.
(3) In the early stage, the recovery of length and width appeared to be parallel processes. The relationship among the rate constants of recovery of area (k_{A1}) length (k_{L1}) and width (k_{W1}) can be approximated as $k_{A1} = k_{L1} + k_{W1}$.
(4) In the later stage of recovery, the length and width appeared to recover consecutively in which the rate constant of area recovery can be expressed as the weighted harmonic mean of those of the length and width recoveries, $1/k_{A2} = L_\infty/(k_{W2}L_{2o}) + W_\infty/(k_{L2}W_{2o})$.
(5) Two types of conformational defects were suggested from this study: one involves large scale chain motions that take place at the earlier stage of recovery; the other involves small scale chain motions that take place at the later stage of the process. These defects carry opposite signs within each category and the recovery involves annihilation of the defect dipoles. Recently, Hahm and Sibener [5] saw some of these defect dipoles in the atomic force microscope.

Table 3
Examination of the rate relationship among k_{A2}, k_{L2} and k_{W2} for the later stage recovery

T (°C)	$1/k_{A2}$ (mm^2 h)	$L_\infty/(k_{W2}L_{2o}) + W_\infty/(k_{L2}W_{2o})$ (mm^2 h)	% difference
106	27,624	32,851	18.9
109	8210	8928	8.7
112	2119	2312	9.1
115	990	1038	4.9
118	245	253	3.3

(6) The two large scale chain motions corresponding to length and width recovery in the early stage appear to operate in parallel, while the two small scale chain motions corresponding to length and width recovery in the later stage occur consecutively one after the other.

Acknowledgements

The authors wish to thank T. Finney for helping with the experiments. The permission from The Dow Chemical Company to publish the work is appreciated.

References

[1] Cleereman KJ, Haram HJ, Williams JC. Mod Plast 1953;30(9):119.
[2] Slone MC, Reinhart FW. Mod Plast 1954;31(10):203.
[3] Chau CC, Rubens LC. Polym Engng Sci 1987;27(14):1095.
[4] Chau CC, Rubens LC, Rieke JK. Polymer 1988;29:99.
[5] Hahm J, Sibener SJ. J Chem Phys 2001;114:4730.
[6] Li JCM. Met Trans 1978;9A:1353.
[7] Chang BTA, Li JCM. J Mater Sci 1980;15:1364.